Environ. Sci. Technol. **2010,** *44,* 3690–3697

Water-Soluble Atmospheric Organic Matter in Fog: Exact Masses and Chemical Formula Identification by Ultrahigh-Resolution Fourier Transform Ion Cyclotron Resonance Mass Spectrometry

LYNN R. MAZZOLENI,*,† BRANDIE M. EHRMANN,‡ XINHUA SHEN,§ ALAN G. MARSHALL,‡,|| AND JEFFREY L. COLLETT, JR.§

Department of Chemistry, Michigan Technological University, 1400 Townsend Drive, Houghton, MI 49931, Department of Chemistry and Biochemistry, Florida State University, 95 Chieftain Way, Tallahassee, FL 32306, Department of Atmospheric Science, Colorado State University, 1371 Campus Delivery, Fort Collins, CO, 80523, and Ion Cyclotron Resonance Program, National High Magnetic Field Laboratory, Florida State University, 1800 East Paul Dirac Drive, Tallahassee, FL 32310-4005

Received November 10, 2009. Revised manuscript received March 9, 2010. Accepted March 25, 2010.

The detailed molecular composition of water-soluble atmospheric organic matter (AOM) contained in fog water was studied by use of electrospray ionization ultrahigh-resolution Fourier transform ion cyclotron resonance mass spectrometry. We identified 1368 individual molecular masses in the range of 100−400 Da from negative-ion spectra obtained after reversed-phase extraction with a hydrophilic solid phase sorbent. The detected organic anions are multifunctional with a variety of oxygenated functional groups. We observe organic nitrogen, organic sulfur, and organic nitrogen−sulfur compounds as well as many species with only C, H, and O elemental composition. Analysis of the double bond equivalents (DBE = the number of rings plus the number of double bonds to carbon) suggests that these compound structures range from highly aliphatic to aromatic with DBE values of 1−11. The compounds range in their extent of oxidation with oxygen to carbon ratios from 0.2 to 2 with an average value of 0.43. Several homologous series of compounds and multifunctional oligomers were identified in this AOM. The high extent of homologous series of compounds likely originates from primary components that have become oxidized. The multifunctional oligomers appear to represent atmospheric processing of primary and secondary compounds. The isolated water-soluble components identified here are amphiphilic, meaning that they contain both hydrophilic oxygenated functional groups and hydrophobic aliphatic and aromatic structural moieties. Despite the high number of compounds with very high oxygen content, 60% of assigned chemical formulas have measured organic mass-to-organic carbon ratios ≤2.25 (ranging from 1.25 to 3.5). Because the results reported here are not quantitative, an average ratio cannot be determined.

Introduction

Atmospheric organic matter (AOM) in the form of organic aerosol or dissolved organic species in suspended cloud or fog droplets is a complex mixture. Its components account for a significant fraction of the total mass of fine particulate matter in the atmosphere (*1*). Early work (*2*) estimated atmospheric water-soluble organic compounds to comprise between 20 and 70% of the total organic aerosol. Identification of water-soluble organic compounds presents a very challenging task. Many have multiple polar functional groups (e.g., carboxyl, hydroxyl, carbonyl, nitro, nitrooxy, and sulfate) and are not well separated by traditional chromatographic techniques. Despite decades of effort water-soluble organic compounds are still not well characterized on a molecular level (*3*). It is desirable to characterize these compounds because they may play essential roles in fundamental environmental processes, such as chemical reduction/oxidation mediation, sorption, complexation, solubilization, and aerosol water-uptake (*4*).

Electrospray ionization coupled with Fourier transform ion cyclotron resonance (FT-ICR) MS provides detailed molecular characterization of organic matter due to its extremely high resolution and mass accuracy (*5*−*7*). ESI is a "soft" ionization technique that offers minimal fragmentation of the analytes, thus allowing for detection of intact molecules (*8*). ESI is especially effective for ionization of polar molecules since ions are typically formed by either protonation or deprotonation of polar moieties (*9*). The ultrahigh resolution of FT-ICR MS has revealed extremely complex mass spectra with up to 63 individual mass peaks per nominal mass (*3, 10*−*12*). Furthermore, the high resolving power of the FT-ICR mass spectrometer provides sufficiently accurate mass measurement for unique assignment of molecular elemental composition of individual components (*13*). This very powerful technique has been used recently by many investigators for identification of complex organic species from a variety of environments (*8, 14*−*21*). In this study, we present molecular level characterization based on FT-ICR MS of isolated water-soluble AOM from radiation fog collected in Fresno, California. Radiation fog droplets form in the surface boundary layer when the atmosphere in contact with the surface rapidly cools, forcing water vapor to condense from the gas phase onto suspended aerosol particles that act as CCN. Fog presents a combination of scavenged particles, water-soluble gases, and their reaction products and therefore defines a rich environment for the study of atmospheric organic matter. Radiation fog events occur during the winter in the central valley of California after several days of stagnant conditions. These stagnant conditions suggest that the aerosol in the valley is a mixture of aged and fresh emissions.

Experimental Methods

Collection of Fog Samples. Fog samples were collected in January 2006 in Fresno, CA. Fog samplers were set up at the California State University experimental farm in an open field in north Fresno. The site was chosen to represent polluted urban fog environment, influenced by emissions from residential, transportation, and industrial activities. Fog

* Corresponding author phone: 906-487-1853; fax: 906-487-2061; e-mail: lrmazzol@mtu.edu.
† Michigan Technological University.
‡ Florida State University.
§ Colorado State University.
|| National High Magnetic Field Laboratory.

10.1021/es903409k
© 2010 American Chemical Society
Published on Web 04/16/2010

samples were collected with a large stainless steel version of the Caltech Active Strand Cloudwater Collector (*22, 23*). The bulk collectors operate by pulling droplet-laden air across a bank of stainless steel strands where cloud/fog drops are collected by inertial impaction. The collected drops flow down into a stainless steel collection trough, through a stainless steel tube, and into a pre-baked glass bottle. The collector operated at a flow rate of ~40 m^3/min, allowing for the collection of large sample volumes. Sampling intervals typically ranged from 1−2 h depending upon the fog liquid water content. A field blank was prepared in the field consisting of high purity water (UV treated and deionized). Samples were filtered immediately after collection with a pre-fired quartz filter. The sample filtrates were stored in pre-baked amber glass jars and refrigerated immediately after analytical aliquots were made. A sample collected on January 6th, 2006 between 12:30 a.m. and 2 a.m. at the beginning of a fog event was selected for the high resolution MS analysis presented here. An aliquot of this sample was analyzed for total and dissolved organic carbon concentrations by use of a Shimadzu TOC-500A analyzer calibrated with potassium hydrogen phthalate. Future publications will present additional samples in time series across single and multiple fog episodes.

FT-ICR MS Sample Preparation. Solid phase extraction (SPE) was used for sample preparation of fog water samples. This method was adapted from Kim et al. (*24*) In this study, we substituted C_{18} disks with a polymeric resin (Phenomenex Strata-X) SPE cartridge. Strata-X is a hydrophilic sorbent made of surface modified styrene-divinylbenzene polymer (similar to XAD-4 resin) with a specific surface area of ~800 m^2/g (*25*). The 1 g SPE cartridges were pre-conditioned with methanol (Fisher Optima grade) and then rinsed with 1% formic acid (Fluka LC/MS grade) in high purity water (UV treated and deionized). A sample volume of 100 mL of previously filtered fog water (with a dissolved organic carbon concentration of 12.7 ppm) was pH adjusted with formic acid to pH 4.5 and then applied to the SPE cartridge at a flow rate of 1 mL/min. After the sample had passed through the cartridge, the cartridge was washed with 1% formic acid in high purity water to remove inorganic compounds. 2 mL of alkaline (pH adjusted to 10.4 with ammonium hydroxide) high-purity water, methanol, and acetonitrile (10/45/45 vol/vol/vol) was used to elute the organic compounds from the SPE cartridge. A brown color band was observed moving down and off the SPE material into the sample vial.

Instrumental Parameters. Samples were analyzed with a hybrid 7 T Fourier transform ion cyclotron resonance (FT-ICR) mass spectrometer (LTQ FT Ultra, Thermo Scientific) equipped with a chip-based direct infusion nanoflow electrospray ionization (nESI) source (Triversa Nanomate, Advion Biosciences, Ithaca, NY). All mass spectra were acquired for negative ions produced by an electrospray source voltage of −1.35 kV and a N_2 gas pressure of 0.35 psi. Selected-ion monitoring (wide SIM mode) allowed isolation of an m/z 600 window in the LTQ before FT-ICR analysis. We used two overlapping windows ($50 < m/z < 650$ and $400 < m/z < 1000$) to cover the full mass range. Mass resolving power, $m/\Delta m_{50\%}$, in which $\Delta m_{50\%}$ is peak full width at half-maximum peak height, was set at 200 000 (at m/z 400) for all spectra. Automatic gain control was used to consistently fill the LTQ with the same number of ions for each acquisition and to avoid space charge effects from over-filling the mass analyzer. The instrument was externally calibrated in negative ion mode with a standard solution of sodium dodecyl sulfate and taurocholic acid, and the resulting mass accuracy was better than 2 ppm. Hundreds of individual mass spectra were collected and stored as transients by use of Thermo Xcalibur software.

Data Processing and Assignment of Elemental Compositions. Approximately 370 transients recorded in the time domain were co-added with Predator v. 3.54.34 (*26*). Co-addition of numerous time domain data sets prior to Fourier transformation enhances the signal-to-noise ratio (*21, 27*). The empirical formula calculator (Sierra Analytics Composer) was used to assign chemical formulas to the masses of singly-charged ions of $100 < m/z < 400$ and relative abundances (RA) ≥1%. The calculator uses the Kendrick mass defect (*28*) to sort homologous ion series (species with a given double bond equivalents (DBE) and heteroatom content but differing by increments of $-CH_2$). The calculator was set to allow up to 30 carbon, 60 hydrogen, 20 oxygen, 3 nitrogen, and 1 sulfur atoms per elemental composition. Naturally present fatty acids were used as internal calibrants (*29*), thereby lowering the average mass error to <0.1 ppm. Data filtering of the assigned formulas was done by applying rules and assumptions as described by Koch and colleagues (*30*). Further information is available in the corresponding Supporting Information (SI). DBE was calculated from eq 1 (*31*):

$$\mathrm{DBE} = c - h/2 + n/2 + 1 \qquad (1)$$

for elemental composition $C_cH_hN_nO_oS_s$. Note that sulfur is divalent in eq 1. Additional bonds formed by tetravalent and hexavalent S are not included in DBE calculations.

Results and Discussion

Mass Spectra and Peak Assignments. With co-addition of ~370 ICR time-domain transients, more than 3000 individually measured masses were observed in the mass to charge ratio (m/z) range of $100 < m/z < 400$. Approximately 10 individual masses were observed within 0.3 Da of each nominal mass (SI Figure S-1). This great complexity observed in atmospheric fog water results from the several sources of AOM including primary components and secondary components formed in either gaseous and/or aqueous secondary reaction pathways. We know from previous studies that even 2−3 component reaction systems can result in hundreds of individually measured masses (*16, 19*). In this study, we analyzed a natural sample with unknown numbers of precursor compounds and a variety of potential reaction pathways. Likewise, Altieri and coworkers (*32*) recently studied rainwater with a similar FT-ICR MS methodology (but without co-addition of transients); they reported elemental compositions for 552 individual masses in the range of 50−500 Da. Previously, Reemtsma et al. (*15*). identified approximately 1000 compounds from $220 < m/z < 420$ and Wozinack et al. (*20*). identified more than 3000 peaks from $223 < m/z < 600$ from aerosol filter samples. These large data sets provide a foundation for understanding the nature of atmospheric AOM, especially with respect to fundamental elemental composition and structural attributes and their changes due to atmospheric chemical transformations. Thus, we include with this paper a complete listing of the assigned chemical formulas and their corresponding measured masses (SI Tables S-1 and S-2).

Overall, 2436 masses were assigned unique elemental compositions. Of those, 1368 "monoisotopic" species contained only the most abundant isotopes (^{12}C, ^{1}H, ^{14}N, ^{16}O, ^{32}S), and the remaining 1068 contained one or more ^{13}C and/or ^{34}S. All assigned ions were singly-charged (as evident from the unit m/z separation between the $^{12}C_c$ and $^{13}C^{12}C_{c-1}$ isotopomers for each elemental composition (*33*)) and even-electron, $[M\text{-}H]^-$ (due to electrospray ionization). We detected the ^{13}C and ^{34}S containing species for 66.5% of the assigned chemical formulas. Most of the remaining 33.5%, without detection of the corresponding ^{13}C masses, were CHNO compounds. However, those compounds belong to Kendrick series (see below)

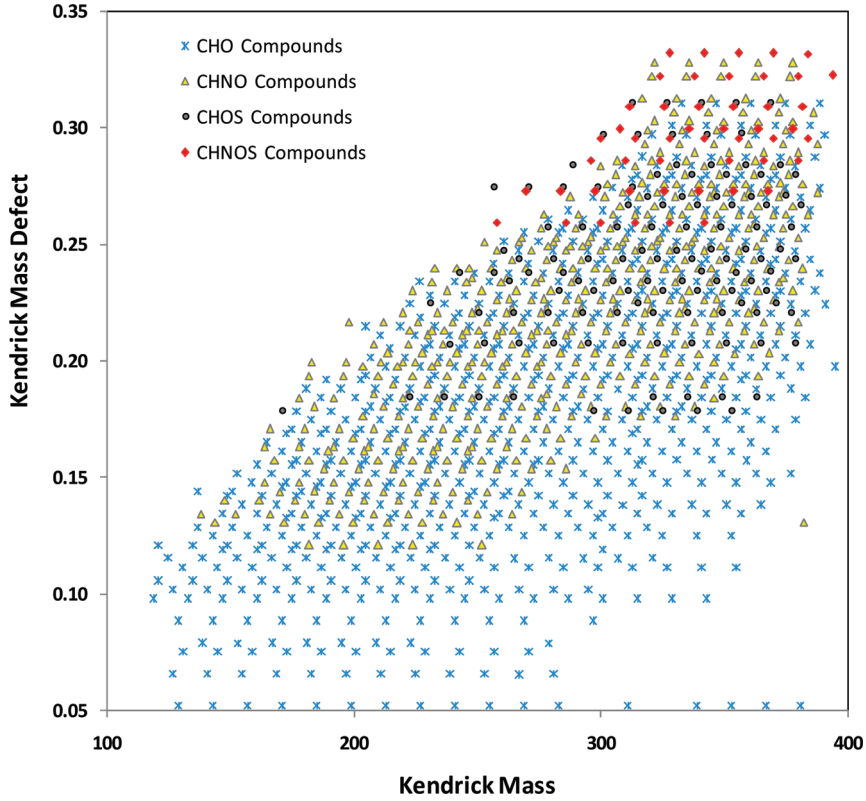

FIGURE 1. The Kendrick mass defect vs. Kendrick nominal mass for 1368 assigned chemical formulas, excluding species containing lesser abundant stable isotopes (^{13}C and ^{34}S). Kendrick mass is previously defined (*21, 28*) as the measured exact mass times the ratio of the nominal to exact mass of CH_2.

for which at least one of the assigned formulas did include a heavy atom to confirm the assignment. Approximately 20% of the total observed mass spectral peaks remain unidentified. Possibly they contain additional elements or more nitrogen or sulfur atoms than permitted in the calculations. Further, because FT-ICR mass measurement precision (*34*) and accuracy (*35*) are directly proportional to peak height-to-noise ratio, it is not possible to obtain unique elemental compositional assignments for the many peaks of low signal-to-noise ratio, especially at the upper end of the mass range. Formula calculations were limited to peaks ≥1% RA;that is, 15 times the peak height-to-noise ratio of 0.0667 % RA. A total of 238 masses were assigned unique elemental compositions in our field blank, with a threshold of 6 times the peak height-to-noise ratio of 0.03 % RA. Of those 238 masses, 83 monoisotopic masses, and 58 isotopomers were in common with the fog water sample. At present it is unclear if the common masses represent nESI-MS carryover from our samples or trace contaminants from laboratory handling. The common masses and chemical formulas are provided in SI Table S-1.

General Characteristics. Based on the chemical formula assignments, we observe low molecular weight AOM compounds with a range of 3−26 carbon atoms per molecule. The most common homologous series found in all natural OM is alkylation (*3*). The homologous series of CH_2 chains are easily revealed by Kendrick mass defect analysis, as in petroleum, for which several CH_2 series span the mass range up to 1500 Da (*28*). Both primary and secondary AOM also contain several homologous series in the range, $100 < m/z < 400$, see the horizontal series of points in the Kendrick plot in Figure 1. Note that these series exist for CHO, CHON, CHOS, and CHNOS compound families. The origin of the high number of homologous series is unknown; however, this observation is consistent with other OM from other natural systems. DBE values determined from the neutral chemical formula range from 1 to 11 (Figure 2A). In addition to the DBE vs. carbon number, we present the analyte RA (i.e., peak height relative to that of the base peak, m/z 183.0047). Note in ESI-MS analysis, relative abundance is the product of initial neutral concentration and ionization efficiency.

Although ionization efficiency can vary among different compounds, we do observe a few similar features between this method and GC/MS methods (*36*). For example, the fatty acid series, (namely, species containing two oxygen atoms and DBE = 1), extends from C_3 to C_{25}, with highest abundance corresponding to palmitic acid (C_{16}) and stearic acid (C_{18}). Long chain alkanoic acids are known to be prevalent in atmospheric aerosols (*37*). Other prominent components (C_{10} and DBE = 2−3) may be monoterpene derivatives. Ions with C_{6-8} and DBE = 5−6 likely correspond to previously observed (*38*) benzoic acid and phenolic structures such as nitrophenols and nitrocresols. Figure 2B displays the number of oxygen atoms vs. the number of carbon for all formulas. It is important to note that DBE counts double bonds to carbon, and thus includes both C═C and C═O species. Decesari et al. suggested that a high percentage of the water-soluble organic compounds associated with aerosol/fog water are polyacidic (*39*). We find up to 10 oxygen atoms in some of our assigned molecular formulas, allowing up to five carboxylic groups. However, due to the observations of organic nitrogen and sulfur in this sample and in previous studies (*40, 41*), it is likely that the AOM is multifunctional with a combination of hydroxyl, carbonyl, carboxyl, ester, nitrate, and sulfate functional groups.

van Krevelen Analysis. The assigned molecular formulas of the AOM are presented in van Krevelen diagrams (*42*), shown in Figures 3 and 4. Each diagram is a plot of the atomic ratio of H:C vs. O:C for each assigned elemental composition. Aliphatic compounds have low O:C ratio (<0.5) and high H:C ratio (>1.5) (upper left). Likewise, aromatic compounds

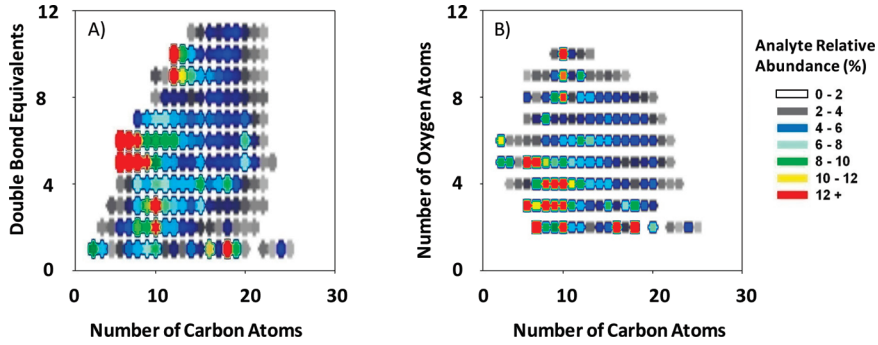

FIGURE 2. Atmospheric organic matter isoabundance contoured plots for 1368 assigned elemental compositions, with color coding for analyte relative abundance (RA) % shown at right. (A) Double bond equivalents versus carbon number, (B) Oxygen number versus carbon number.

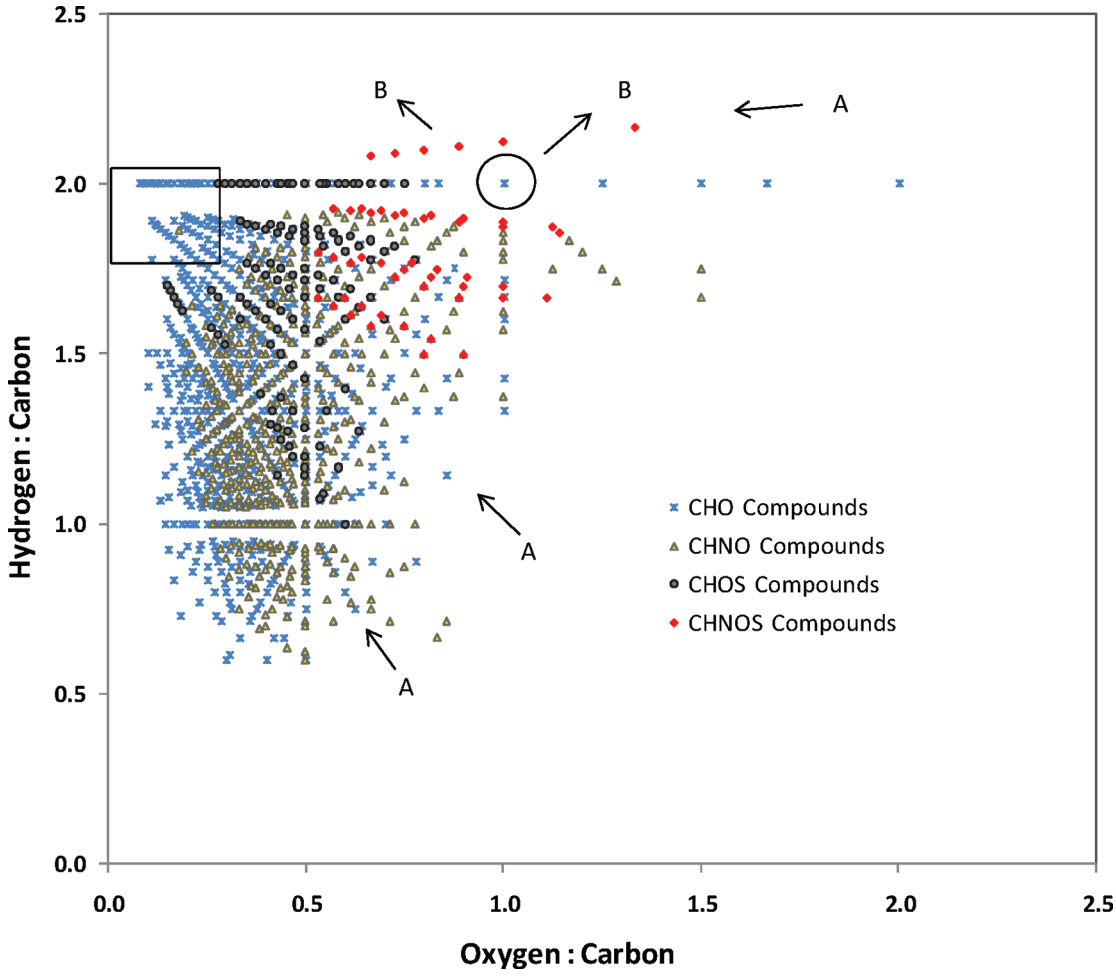

FIGURE 3. van Krevelen plot of h:c vs. o:c ratio for 1368 assigned elemental compositions, $C_cH_hO_oN_nS_s$, without relative abundance coding. (A) Aliphatic homologous series (CH_2 groups) are distinguished by diagonal lines relative to the upper left box (diagonal-A). A few selected homologous series are shown with the arrow pointing in the direction of chain elongation. (B) Compounds related to each other (within a group) by multiples of CH_2O are distinguished by the diagonal lines relative to the upper right oval (diagonal-B). A few selected condensation/dehydration series are shown with the arrow indicating the direction of chain elongation.

typically exhibit low O:C ratio (<0.5) and low H:C ratio (<1.0) (lower left). Further, van Krevelen plots are used to evaluate the degree of alkylation, hydrogenation, hydration, and oxidation of AOM (*7, 43*). However, it is important to note that although a typical compound family may occupy a defined area in a van Krevelen plot, the converse is *not* true, that is, location of an unknown compound in the same region does *not* prove that it belongs to that compound family.

As described by Kim et al. (*43*), distinctive lines in the plot can represent chemical trends within a compound group. Several lines (horizontal, vertical, and diagonal) similar to plots for organic matter from aquatic environments (*43*) are shown in Figure 3. These lines can reflect compound relationships such as oxidation/reduction (horizontal), hydrogenation (vertical), alkylation (diagonal-A) and condensation (diagonal-B). As expected from the number of homologous series in the Kendrick plot (Figure 2), the data shown in Figure 3 exhibit pronounced diagonal-A lines (relative to the box in the upper left portion of the plot). In addition, several diagonal-B lines are seen relative to the oval in the upper right portion of the plot. These compound

relationships occur for many processes, and thus can provide clues regarding the nature of the primary and secondary organic aerosol simultaneously.

The chemical trends are further elucidated with abundance-weighted van Krevelen plots (Figure 4). Figure 4A includes all of the assigned chemical formulas whereas Figures 4B−D include those compositions containing only CHO, CHNO, and CHOS, and/or CHNOS compounds. Although diagonal-A lines are prominent in Figure 4C and D, diagonal-B lines are not easily distinguished in the abundance-weighted van Krevelen plots of Figure 4. The prominence of the diagonal-A lines indicates an aliphatic predominance. The observed aliphatic character cannot be explained solely by the presence of alkanoic mono- and dicarboxylic acids, but must also be in the form of alkyl substituents, as indicated by the range of DBE values and other elements (N and S).

A total of 715 of the exact mass measurements could be assigned to elemental compositions containing only C, H, and O, presumably including carbonyl, carboxyl, and/or hydroxyl functional groups. From the van Krevelen diagram in Figure 4B, we observe a high-abundance cluster spanning $0.2 < O:C < 1.0$ and $0.5 < H:C < 2.0$. In general, the compounds appear to be significantly oxidized with an average O:C ratio of ~0.5. The observed O:C and H:C ratios are higher than those from van Krevelen diagrams of dissolved organic matter (DOM) from surface water (*44*). In other studies of AOM (*32, 20*), the observed atomic ratio ranges are similar for CHO compounds, although Wozniak and co-workers (*20*) found many lower O:C ratios (0.1−0.8) in their aerosol samples than observed here for fogwater AOM or by Altieri et al. (*32*) in rainwater AOM (approximately 0.1−2.0). That difference is not surprising, given the tendency of atmospheric water to be enriched in more polar compounds relative to atmospheric particulate matter. None of the observations of AOM (previous studies *32, 20* and this study), report a particularly high number of aromatic compounds, determined by a low H:C ratio.

Aqueous secondary organic aerosol oligomer products of CHO compounds have been reported recently by Alteri et al. (*32*), The oligomers were reported to form by an esterification reaction resulting in a mass increase of $C_3H_4O_2$ (*16*). In our study, we observe only a few of the same oligomer product masses (*32*) (SI Table S-1). However, by re-scaling our Kendrick masses to identify homologous series differing by multiples of $C_3H_4O_2$ (*42, 43*)

$$\text{Kendrick mass } (C_3H_4O_2) = \text{observed mass} \times \frac{\text{nominal mass of } C_3H_4O_2}{\text{exact mass of } C_3H_4O_2} \quad (2)$$

$$\text{Kendrick mass defect } (C_3H_4O_2) = |\text{nominal mass} - \text{kendrick mass } (C_3H_4O_2)| \quad (3)$$

we did find many other compounds resulting from the esterification reaction mechanism reported in Altieri et al. (*32*).

In this way, we identified 238 individual oligomer series of two to four compounds separated by multiples of $C_3H_4O_2$ within our CHO subset of assigned molecular formulas. This high number of oligomer series represents 88% of the number of CHO assignments. The structural elucidations from that analysis will be presented in a future publication.

A high level of organic nitrogen in California fog waters (*45, 46*) and in New Jersey rainwater (*47*) has been reported previously. Here, we assigned 487 molecular formulas containing nitrogen. As shown in Figure 4C, these compounds represent a substantial fraction of the integrated mass spectral signal. Most occur in the same O:C and H:C range as the CHO compounds, and appear to be aliphatic or include alkyl substituents as noted by the occurrence of diagonal-A lines. The CHNO group consists of 13 compound subgroups denoted by variation in nitrogen and oxygen atoms: NO_3 − NO_9, N_2O_5 − N_2O_9, and N_3O_8. The high number of oxygen and nitrogen atoms suggests that these compounds are multifunctional with up to three nitro and/or nitrooxy functional groups in addition to other polar functional groups mentioned previously. A high number of species with nitrooxy functional groups has been observed elsewhere (*32*). Evidence for secondary organic aerosol formation by NO_x reactions has been presented previously (*48*). The mechanism was described as an addition of NO_3 to a carbon−carbon double

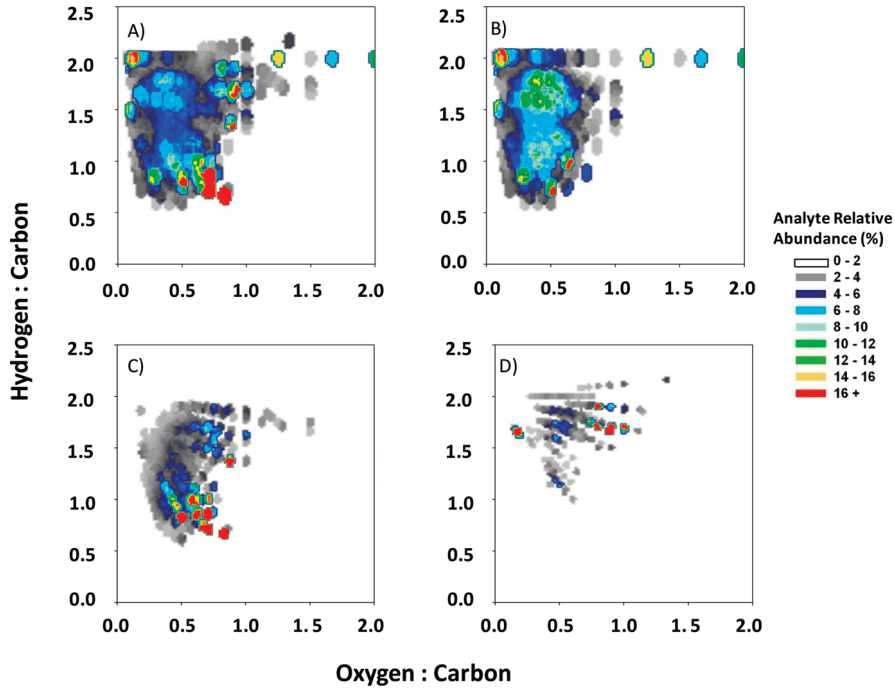

FIGURE 4. van Krevelen plots with color-coded analyte relative abundance (right); (A) all 1,368 $C_cH_hO_oN_nS_s$ compositions; (B) 715 compounds containing only C, H, and O atoms; (C) 487 compounds containing only C, H, N, and O atoms; and (D) 166 compounds containing only C, H, O, and S or C, H, N, O, and S atoms.

bond with subsequent addition of O_2. Thus it was suggested that a variety of nitrated organic compounds, including hydroxynitrates, carbonyl nitrates, dinitrates, hydroxydinitrates, and other highly nitrated compounds, could be formed.

The CHNO compounds span a wide DBE range (3−11), indicating a high prevalence of double bonds and/or ring structures. Examination of the DBE vs. carbon number indicates that the most abundant CHNO species exhibit DBE = 5, 6, 9, and 10 (SI Figure S-2), likely corresponding to mono- and di-nitro substituted phenols, cresols, benzoic acids, and naphthalenes. In a recent review (*38*) of nitrophenols, concentrations of up to 40 μg/L for both 4-nitrophenol and 2,4-dinitrophenol were reported in fog. Within the CHNO group, we found 145 oligomer series of 2−3 compounds, representing 71% of the number of assigned CHNO chemical formulas.

We also assigned 168 different organic sulfur elemental compositions. The CHOS and CHNOS compounds are shown in a van Krevelen diagram (Figure 4D). Most show 0.2 < O:C < 1.2 and 1 < H:C < 2.1, as for the CHO compounds: namely, aliphatic with a low degree of oxidation. The four most prominent individual negative ions in this group are $C_{16}H_{25}O_3S^-$, $C_{17}H_{27}O_3S^-$, $C_{18}H_{29}O_3S^-$, $C_{19}H_{31}O_3S^-$ corresponding to m/z 297.15298, 311.1587, 325.1844, and 339.2000. These compounds are 4 of 6 in a Kendrick series of SO_3 compounds with DBE = 4, and C_{7-20}. Those four compounds have been observed previously (*32*) and are suspected to be synthetic linear alkylbenzene sulfonates. The identical masses were also observed for the field blank (SI Tables S-1 and S-2), although with much lower ion abundances.

The oxygen number for each of the remaining CHOS and CHNOS compounds was 5 or more, suggesting that most of them are multifunctional with sulfate groups. In 2005, Romero and Oehme (*40*) reported observations of organosulfates at m/z 229, 265, 279, and 299 based on nominal mass accuracy. Our assigned chemical formulas are consistent with organosulfates at several of these and other masses. For example, we observe two species near m/z 265 and 279, $C_{10}H_{17}O_6S^-$, $C_{11}H_{21}O_5S^-$, $C_{10}H_{15}O_7S^-$, and $C_{11}H_{19}O_6S^-$ whose neutral precursors have DBE values of 2, 1, 3, and 2. Additional observations of organosulfates have been made by Surratt et al. (*49*), in their study of secondary organic aerosol formation via ozonolysis of biogenic hydrocarbons. We found a few of the same masses ($C_{10}H_{15}O_7S^-$, $C_{10}H_{17}O_7S^-$, and $C_{10}H_{19}O_7S^-$) (SI Table S-1). We have also identified several oligomers: 4 series in the CHNOS group and 18 series in the CHOS group. Due to the higher mass of these molecules, the oligomerization series range from 2 to 3 compounds each. The oligomers represent 16 and 32% of the number of assigned molecular formulas of the CHNOS and CHOS families.

In general, the overall trend for the CHOS and CHNOS compounds is that of the alkylation and de-alkylation lines (diagonal-A). It is unclear why the increasing or decreasing chain length trends appear in each of the above described plots, especially Figure 4C and D. It may be related to the random nature of oxidation reactions or a high occurrence of aliphatic biopolymers in the atmosphere. In a recent paper, Gómez-González and colleagues (*17*) observed organosulfates that appear to originate from photooxidation of unsaturated fatty acids. Given the apparent trend of alkylation in the CHOS graph, we suspect that many of the presently identified organic sulfur compounds may also originate from oxidation of aliphatic compounds such as alkenes and alkenoic acids. Other CHOS and CHNOS compounds correspond to α- and β-pinene oxidation products. Iinuma and coworkers (*50*) observed several nitroxy-organosulfates in nighttime (but not daytime) ambient samples collected in a forested site in northern Germany. One of the masses corresponds to nitro-organosulfates observed by Iinuma et al. (*50*). and Surratt et al. (*49*). was observed at high relative abundance in our nighttime fog sample; m/z 342.05004 (DBE = 3) corresponding to $C_{10}H_{16}NO_{10}S^-$. A few abundant members of this group are $C_{10}H_{16}NO_9S^-$, $C_9H_{14}NO_8S^-$, $C_{10}H_{18}NO_8S^-$, $C_{10}H_{16}NO_8S^-$, and $C_{12}H_{20}NO_9S^-$, with neutral precursor DBE values of 3, 3, 2, 3, and 3. Those compounds appear to be oxidized monoterpenes and may have formed in a manner similar to those observed in chamber studies (*17, 50*).

Atmospheric Implications. The isolated water-soluble AOM identified in fog water was found to be quite complex with a range of O:C ratios from 0.2 to 2.0 and DBE values from 1 to 11. As expected, these components also have variable mass ratios for organic matter to organic carbon (also known as organic mass to organic carbon ratio (OM/OC) (*51*)) ranging from 1.25 to 3.5 (SI Figure S-3). Consistent with previous studies (*16, 32*), we define OM/OC as the measured mass divided by the calculated mass of carbon in the assigned formulas. Despite the high number of compounds with very high oxygen content 60% of assigned chemical formulas have OM/OC ratios ≤2.25. Since the results reported here are not quantitative, an average OM/OC ratio for mass closure (*51, 52*) cannot be determined. It is important to note that fog scavenging of AOM and nESI MS analysis are both likely to favor identification of hydrophilic and neutral polar compounds with higher than average OM/OC ratio. At the same time, the urban location (close to sources) and winter period (low oxidant concentrations) of the sampling period do not favor extensive oxidation of AOM which would typically increase the observed OM/OC ratio. A histogram of the individually measured OM/OC values is provided in SI Figure S-3.

The isolated water-soluble AOM identified in this study appears to result from oxidized variations of aliphatic and aromatic precursor compounds. The oxidized precursors undergo esterification reactions to form a high number of oligomer products. In this work, we found 406 individual oligomer series, accounting for a very high percentage of the CHO and CHNO assigned formulas. The origin of the highly prevalent CH_2 homologous series remains unknown. Because the oligomerization reactions (*16*) change the ratio of elements, the oligomers will have a different Kendrick (CH_2) mass defect. Note that each homologous series identified here varies in length from 5 to 18 carbon atoms. The high occurrence of homologous series observed here could result from the oxidation of primary aliphatic components from biopolymers as hypothesized by Poschl (*53*) and observed in Fresno fog water previously (*54*). Further work is needed to identify the primary reaction pathways involving additional types of primary aerosol and bio-aerosol.

Acknowledgments

We thank Dr. Charles Krauter of California State University Fresno for providing us with field and lab space for fog collection and sample preparation. We thank Drs. Melissa Soule and Elizabeth Kujawinski of the Woods Hole Oceanographic Institution Mass Spectrometry Facility for instrument time and data acquisition (NSF OCE-0619608 and Gordon and Betty Moore Foundation). A.G.M. and B.E. were supported by the NSF Division of Materials Research (DMR-0654118) and the State of Florida. Other major research funding for this work was provided by the NSF Division of Atmospheric Chemistry (ATM-0222607, ATM-0521643) and through a Los Alamos National Laboratory, Institute of Geophysics and Planetary Physics Mini-grant Award. L.R.M. gratefully acknowledges partial support from a joint postdoctoral fellowship between Colorado State University and the Cooperative Institute for Research in the Atmosphere.

Supporting Information Available

A compact list of all assigned molecular formulas, DBE values, MS relative abundances, and compound classes is provided. Additional figures for data visualization are also provided. Additional data may be provided upon request. This material is free of charge via the internet at http://pubs.acs.org.

Literature Cited

(1) Fuzzi, S.; Andreae, M. O.; Huebert, B. J.; Kulmala, M.; Bond, T. C.; Boy, M.; Doherty, S. J.; Guenther, A.; Kanakidou, M.; Kawamura, K.; Kerminen, V. M.; Lohmann, U.; Russell, L. M.; Poschl, U. Critical assessment of the current state of scientific knowledge, terminology, and research needs concerning the role of organic aerosols in the atmosphere, climate, and global change. *Atmos. Chem. Phys.* **2006**, *6*, 2017–2038.

(2) Saxena, P.; Hildemann, L. M. Water-soluble organics in atmospheric particles: A critical review of the literature and application of thermodynamics to identify candidate compounds. *J. Atmos. Chem.* **1996**, *24* (1), 57–109.

(3) Reemtsma, T. Determination of molecular formulas of natural organic matter molecules by (ultra-) high-resolution mass spectrometry status and needs. *J. Chromatogr., A* **2009**, *1216* (18), 3687–3701.

(4) Graber, E. R.; Rudich, Y. Atmospheric HULIS: How humic-like are they? A comprehensive and critical review. *Atmos. Chem. Phys.* **2006**, *6*, 729–753.

(5) Marshall, A. G.; Hendrickson, C. L.; Jackson, G. S. Fourier transform ion cyclotron resonance mass spectrometry: A primer. *Mass Spectrom. Rev.* **1998**, *17*, 1–17.

(6) Kujawinski, E. B. Electrospray ionization fourier transform ion cyclotron resonance mass spectrometry (ESI FT-ICR MS): Characterization of complex environmental mixtures. *Environ. Forensics* **2002**, *3* (3−4), 207–216.

(7) Sleighter, R. L.; Hatcher, P. G. The application of electrospray ionization coupled to ultrahigh resolution mass spectrometry for the molecular characterization of natural organic matter. *J. Mass Spectrom.* **2007**, *42* (5), 559–574.

(8) Stenson, A. C.; Landing, W. M.; Marshall, A. G.; Cooper, W. T. Ionization and fragmentation of humic substances in electrospray ionization fourier transform-ion cyclotron resonance mass spectrometry. *Anal. Chem.* **2002**, *74* (17), 4397–4409.

(9) Gaskell, S. J. Electrospray: Principles and practice. *J. Mass Spectrom.* **1997**, *32* (7), 677–688.

(10) Grannas, A. M.; Hockaday, W. C.; Hatcher, P. G.; Thompson, L. G.; Mosley-Thompson, E. New revelations on the nature of organic matter in ice cores. *J. Geophys. Res., [Atmos.]* **2006**, *111zissD4*.

(11) Purcell, J. M.; Hendrickson, C. L.; Rodgers, R. P.; Marshall, A. G. Atmospheric pressure photoionization fourier transform ion cyclotron resonance mass spectrometry for complex mixture analysis. *Anal. Chem.* **2006**, *78* (16), 5906–5912.

(12) Marshall, A. G.; Rodgers, R. P. Petroleomics: Chemistry of the underworld. *Poc. Natl. Acad. Sci. U.S.A.* **2008**, *105* (47), 18090–18095.

(13) Kim, S.; Rodgers, R. P.; Marshall, A. G. Truly "exact" mass: elemental composition can be determined uniquely from molecular mass measurement at similar to 0.1 mDa accuracy for molecules up to similar to 500 Da. *Int. J. Mass Spectrom.* **2006**, *251* (2−3), 260–265.

(14) Kujawinski, E. B.; Freitas, M. A.; Zang, X.; Hatcher, P. G.; Green-Church, K. B.; Jones, R. B. The application of electrospray ionization mass spectrometry (ESI MS) to the structural characterization of natural organic matter. *Org. Geochem.* **2002**, *33* (3), 171–180.

(15) Reemtsma, T.; These, A.; Venkatachari, P.; Xia, X. Y.; Hopke, P. K.; Springer, A.; Linscheid, M. Identification of fulvic acids and sulfated and nitrated analogues in atmospheric aerosol by electrospray ionization fourier transform ion cyclotron resonance mass spectrometry. *Anal. Chem.* **2006**, *78* (24), 8299–8304.

(16) Altieri, K. E.; Seitzinger, S. P.; Carlton, A. G.; Turpin, B. J.; Klein, G. C.; Marshall, A. G. Oligomers formed through in-cloud methylglyoxal reactions: Chemical composition, properties, and mechanisms investigated by ultra-high resolution FT-ICR mass spectrometry. *Atmos. Environ.* **2008**, *42* (7), 1476–1490.

(17) Gomez-Gonzalez, Y.; Surratt, J. D.; Cuyckens, F.; Szmigielski, R.; Vermeylen, R.; Jaoui, M.; Lewandowski, M.; Offenberg, J. H.; Kleindienst, T. E.; Edney, E. O.; Blockhuys, F.; Van Alsenoy, C.; Maenhaut, W.; Claeys, M. Characterization of organosulfates from the photooxidation of isoprene and unsaturated fatty acids in ambient aerosol using liquid chromatography/(−) electrospray ionization mass spectrometry. *J. Mass Spectrom.* **2008**, *43* (3), 371–382.

(18) Hughey, C. A.; Rodgers, R. P.; Marshall, A. G. Resolution of 11 000 compositionally distinct components in a single electrospray ionization fourier transform ion cyclotron resonance mass spectrum of crude oil. *Anal. Chem.* **2002**, *74* (16), 4145–4149.

(19) Reinhardt, A.; Emmenegger, C.; Gerrits, B.; Panse, C.; Dommen, J.; Baltensperger, U.; Zenobi, R.; Kalberer, M. Ultrahigh mass resolution and accurate mass measurements as a tool to characterize oligomers in secondary organic aerosols. *Anal. Chem.* **2007**, *79* (11), 4074–4082.

(20) Wozniak, A. S.; Bauer, J. E.; Sleighter, R. L.; Dickhut, R. M.; Hatcher, P. G. Technical note: Molecular characterization of aerosol-derived water soluble organic carbon using ultrahigh resolution electrospray ionization fourier transform ion cyclotron resonance mass spectrometry. *Atmos. Chem. Phys.* **2008**, *8* (17), 5099–5111.

(21) Stenson, A. C.; Marshall, A. G.; Cooper, W. T. Exact masses and chemical formulas of individual Suwannee river fulvic acids from ultrahigh resolution electrospray ionization fourier transform ion cyclotron resonance mass spectra. *Anal. Chem.* **2003**, *75* (6), 1275–1284.

(22) Herckes, P.; Lee, T.; Trenary, L.; Kang, G. G.; Chang, H.; Collett, J. L. Organic matter in central california radiation fogs. *Environ. Sci. Technol.* **2002**, *36* (22), 4777–4782.

(23) Herckes, P.; Hannigan, M. P.; Trenary, L.; Lee, T.; Collett, J. L., Jr. Organic compounds in radiation fogs in Davis (California). *Atmos. Res.* **2002**, *64* (1−4), 99–108.

(24) Kim, S.; Simpson, A. J.; Kujawinski, E. B.; Freitas, M. A.; Hatcher, P. G. High resolution electrospray ionization mass spectrometry and 2D solution NMR for the analysis of DOM extracted by C-18 solid phase disk. *Org. Geochem.* **2003**, *34* (9), 1325–1335.

(25) Fontanals, N.; Marce, R. M.; Borrull, F. New hydrophilic materials for solid-phase extraction. *Trends Anal. Chem.* **2005**, *24* (5), 394–406.

(26) Blakney, G. T.; Robinson, D. E.; Ly, N. V.; Kelleher, N. L.; Hendrickson, C. L.; Marshall, A. G. Predator: PCI Data Station for FT-ICR Mass Spectrometry. In *53rd American Society of Mass Spectrometry Annual Conference on Mass Spectrometry & Allied Topics*, San Antonio, TX, June 4−9, 2005.

(27) Kujawinski, E. B.; Hatcher, P. G.; Freitas, M. A. High-resolution fourier transform ion cyclotron resonance mass spectrometry of humic and fulvic acids: Improvements and comparisons. *Anal. Chem.* **2002**, *74* (2), 413–419.

(28) Hughey, C. A.; Hendrickson, C. L.; Rodgers, R. P.; Marshall, A. G.; Qian, K. N. Kendrick mass defect spectrum: A compact visual analysis for ultrahigh-resolution broadband mass spectra. *Anal. Chem.* **2001**, *73* (19), 4676–4681.

(29) Sleighter, R. L.; McKee, G. A.; Liu, Z.; Hatcher, P. G. Naturally present fatty acids as internal calibrants for fourier transform mass spectra of dissolved organic matter. *Limmol. Oceangr., Methods* **2008**, *6*, 246–253.

(30) Koch, B. P.; Witt, M. R.; Engbrodt, R.; Dittmar, T.; Kattner, G. Molecular formulae of marine and terrigenous dissolved organic matter detected by electrospray ionization fourier transform ion cyclotron resonance mass spectrometry. *Geochim. Cosmochim. Acta* **2005**, *69* (13), 3299–3308.

(31) McLafferty, F. W.; Turecek, F., *Interpretation of Mass Spectra*, 4th ed.; University Science Books: Sausalito, CA, 1993; p 371.

(32) Altieri, K. E.; Turpin, B. J.; Seitzinger, S. P. Oligomers, organosulfates, and nitrooxy organosulfates in rainwater identified by ultra-high resolution electrospray ionization FT-ICR mass spectrometry. *Atmos. Chem. Phys.* **2009**, *9* (7), 2533–2542.

(33) Senko, M. W.; Beu, S. C.; McLafferty, F. W. Automated assignment of charge states from resolved isotopic peaks for multiply charged ions. *J. Am. Soc. Mass Spectrom.* **1995**, *6* (1), 52–56.

(34) Chen, L. C.; Cottrell, C. E.; Marshall, A. G. Effect of signal-to-noise ratio and number of data points upon precision in measurement of peak amplitude, position and width in fourier-transform spectrometry. *Chemom. Intell. Lab. Syst.* **1986**, *1* (1), 51–58.

(35) Yanofsky, C. M.; Bell, A. W.; Lesimple, S.; Morales, F.; Lam, T. T.; Blakney, G. T.; Marshall, A. G.; Carrillo, B.; Lekpor, K.; Boismenu, D.; Kearney, R. E. Multicomponent internal recalibration of an LC-FTICR-MS analysis employing a partially characterized complex peptide mixture: Systematic and random errors. *Anal. Chem.* **2005**, *77* (22), 7246–7254.

(36) Rinehart, L. R.; Fujita, E. M.; Chow, J. C.; Magliano, K.; Zielinska, B. Spatial distribution of $PM_{2.5}$ associated organic compounds in central california. *Atmos. Environ.* **2006**, *40* (2), 290–303.

(37) Simoneit, B. R. T. Organic-matter in eolian dusts over Atlantic Ocean. *Mar. Chem.* **1977**, *5* (4−6), 443–464.
(38) Harrison, M. A. J.; Barra, S.; Borghesi, D.; Vione, D.; Arsene, C.; Olariu, R. L. Nitrated phenols in the atmosphere: A review. *Atmos. Environ.* **2005**, *39* (2), 231–248.
(39) Decesari, S.; Facchini, M. C.; Fuzzi, S.; Tagliavini, E. Characterization of water-soluble organic compounds in atmospheric aerosol: A new approach. *J. Geophys. Res., Atmos.* **2000**, *105* (D1), 1481–1489.
(40) Romero, F.; Oehme, M. Organosulfates—A new component of humic-like substances in atmospheric aerosols. *J. Atmos. Chem.* **2005**, *52* (3), 283–294.
(41) Reemtsma, T.; These, A.; Venkatachari, P.; Xia, X.; Hopke, P. K.; Springer, A.; Linscheid, M. Identification of fulvic acids and sulfated and nitrated analogues in atmospheric aerosol by electrospray ionization fourier transform ion cyclotron resonance mass spectrometry. *Anal Chem* **2006**, *78* (24), 8299–8304.
(42) Wu, Z. G.; Rodgers, R. P.; Marshall, A. G. Two- and three-dimensional van krevelen diagrams: A graphical analysis complementary to the kendrick mass plot for sorting elemental compositions of complex organic mixtures based on ultrahigh-resolution broadband fourier transform ion cyclotron resonance mass measurements. *Anal. Chem.* **2004**, *76* (9), 2511–2516.
(43) Kim, S.; Kramer, R. W.; Hatcher, P. G. Graphical method for analysis of ultrahigh-resolution broadband mass spectra of natural organic matter, the Van Krevelen diagram. *Anal. Chem.* **2003**, *75* (20), 5336–5344.
(44) Kim, S.; Kaplan, L. A.; Hatcher, P. G. Biodegradable dissolved organic matter in a temperate and a tropical stream determined from ultra-high resolution mass spectrometry. *Limmol. Oceanogr.* **2006**, *51* (2), 1054–1063.
(45) Zhang, Q.; Anastasio, C. Chemistry of fog waters in California's Central Valley—Part 3: Concentrations and speciation of organic and inorganic nitrogen. *Atmos. Environ.* **2001**, *35* (32), 5629–5643.
(46) Herckes, P.; Leenheer, J. A.; Collett, J. L. Comprehensive characterization of atmospheric organic matter in Fresno, California fog water. *Environ. Sci. Technol.* **2007**, *41* (2), 393–399.
(47) Altieri, K. E.; Turpin, B. J.; Seitzinger, S. P. Composition of dissolved organic nitrogen in continental precipitation investigated by ultra-high resolution FT-ICR mass spectrometry. *Environ. Sci. Technol.* **2009**, *43* (18), 6950–6955.
(48) Docherty, K. S.; Ziemann, P. J. Reaction of oleic acid particles with NO_3 radicals: Products, mechanism, and implications for radical-initiated organic aerosol oxidation. *J. Phys. Chem., A* **2006**, *110* (10), 3567–3577.
(49) Surratt, J. D.; Gomez-Gonzalez, Y.; Chan, A. W. H.; Vermeylen, R.; Shahgholi, M.; Kleindienst, T. E.; Edney, E. O.; Offenberg, J. H.; Lewandowski, M.; Jaoui, M.; Maenhaut, W.; Claeys, M.; Flagan, R. C.; Seinfeld, J. H. Organosulfate formation in biogenic secondary organic aerosol. *J. Phys. Chem., A* **2008**, *112* (36), 8345–8378.
(50) Iinuma, Y.; Muller, C.; Berndt, T.; Boge, O.; Claeys, M.; Herrmann, H. Evidence for the existence of organosulfates from beta-pinene ozonolysis in ambient secondary organic aerosol. *Environ. Sci. Technol.* **2007**, *41*, 6678–6683.
(51) El-Zanan, H. S.; Lowenthal, D. H.; Zielinska, B.; Chow, J. C.; Kumar, N. Determination of the organic aerosol mass to organic carbon ratio in improve samples. *Chemosphere* **2005**, *60* (4), 485–496.
(52) El-Zanan, H. S.; Zielinska, B.; Mazzoleni, L. R.; Hansen, D. A. Analytical determination of the aerosol organic mass-to-organic carbon ratio. *J. Air Waste Manage. Assoc.* **2009**, *59* (1), 58–69.
(53) Poschl, U. Atmospheric aerosols: Composition, transformation, climate and health effects. *Angew. Chem., Int. Ed.* **2005**, *44* (46), 7520–7540.
(54) Herckes, P.; Leenheer, J. A.; Collett, J. L., Jr. Comprehensive characterization of atmospheric organic matter in Fresno, California fog water. *Environ. Sci. Technol.* **2007**, *41* (2), 393–399.

ES903409K